

# TOP ELECTRODE SHAPING FOR HARNESSING HIGH COUPLING IN THICKNESS SHEAR MODE RESONATORS IN Y-CUT LITHIUM NIOBATE THIN FILMS

Abhay Kochhar, Gabriel Vidal-Álvarez, Luca Colombo, and Gianluca Piazza  
Carnegie Mellon University, Pittsburgh, USA

## ABSTRACT

This paper reports a novel electrode shape for harnessing the high electromechanical coupling of the thickness shear mode (TSM) in Y-cut lithium niobate (LN) thin film resonators. To maximize the coupling, we follow Mindlin's [1-3] work, which uses two-dimensional equations of motion with transverse shear deformations to determine the most appropriate electrode shape for an anisotropic plate. We experimentally demonstrate an electromechanical coupling ( $k_t^2$ ) of  $\sim 37\%$ , which agrees well with 3D COMSOL finite elemental method (FEM) simulations. Such high coupling resonators could find application in reconfigurable RF systems.

## INTRODUCTION

Quartz based TSM resonators have been used for sensing and timing applications because of their high quality factor ( $Q$ ). If larger electromechanical couplings were available, the application of TSM resonators could be extended to RF components and especially reconfigurable filters. Thin films such as AlN, ZnO, and PZT have been used to implement shear mode resonators on silicon [4-6]. Nonetheless, their coupling coefficients are limited or require impractical electrode placements to excite the device into vibrations. LN has a trigonal symmetry, and depending on the crystalline cut, various types of acoustic modes can be excited for a wide range of applications. Kuznetsova [7] first reported on the ability to excite various modes in thin films of LN and lithium tantalate (LT) using interdigitated electrodes (IDE) placed on the top surface of these thin films. Recently, LN and LT have become available in thin films on silicon or other carrier wafers and have been excited in various modes by means of IDEs [8-10]. Efficient excitation of thickness shear mode resonators (TSM) requires sandwiching the films between two electrodes. This has been more challenging for thin films of LN and LT and was only attempted for the first time in [10] with Y-cut LN. In [10] the devices suffered from large spurious modes and attained coupling far from the theoretical maximum of  $\sim 37\%$ . As LN is an anisotropic material, conventional electrode shapes (bar, square, circular, ring, etc.) do not properly confine the energy in the resonator. In this paper, we present how shaping the electrode and top surface of the TSM resonator enables coupling coefficients close to the theoretical limit.

## THICKNESS SHEAR RESONATOR DESIGN

Electrode shaping is critical in the design of any piezoelectric resonators. Thickness shear modes in quartz crystals have been extensively studied by Mindlin and others [11]. In this previous work, the anisotropy of the piezoelectric material was taken into account. The key

conclusion of these investigations is that thickness-shear modes do not exist in a pure form in a bounded plate because the presence of any boundaries (such as anchors or resonator edges) results in the excitation of harmonics of flexural modes. Various types of techniques to isolate the thickness-shear mode and suppress flexural modes have been demonstrated for quartz crystals. To name some of the most relevant – beveling, contouring, mass-loading or energy trapping by electrode shaping – have been implemented. These techniques have been successful on macroscale prototypes working in the MHz range. Thanks to microfabrication techniques, we can reproduce some of these methods into high frequency devices made out of LN, hence harnessing the full capabilities of these thin films.

## Rectangular shape electrode

The rectangular shape electrode, which was previously used to excite TSM in a LN plate [10], failed to effectively couple into the desired mode resulting in an electromechanical coupling coefficient  $< 21\%$ . Split modes around the main resonance were recorded. To understand whether these modes are intrinsic to the way the TSM was excited we performed 3D COMSOL FEM analysis of such devices scaled for thicker films. A  $2.5 \mu\text{m}$  LN thin film with top electrode of 100 nm aluminum and bottom electrode of 100 nm platinum (Pt) forms the device stack. The LN thickness was selected to operate around 650 MHz. The electrode thicknesses were chosen given the fabrication constraints and the desire to minimize mass loading. In the FEM analysis, a perfectly matched layer (PML) boundary condition is used to model energy loss due to acoustic energy leaking in the surrounding substrate.

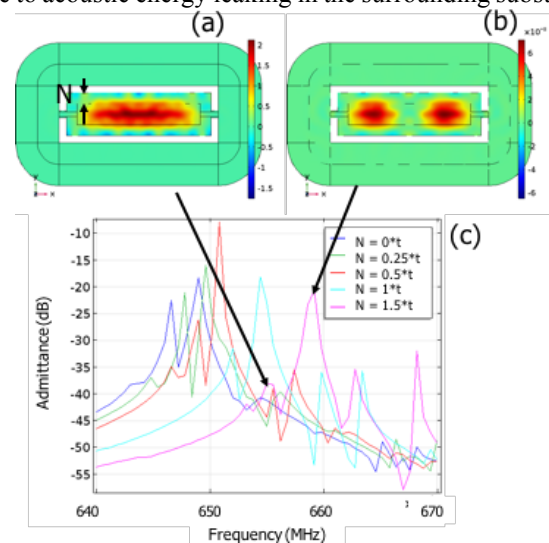


Figure 1: Simulated admittance response of the TSM resonator formed by a rectangular top electrode. (a) Main TSM mode, (b) split mode, (c) admittance plot showing how the split mode is present despite changes in electrode coverage.

We investigated how the split mode depends on the electrode coverage by varying the spacing between the electrode edge and resonator edge (defined by  $N \cdot t$ , where  $N$  was made to vary between 0 and 1.5 and  $t$  is the LN thickness, which is approximately equal to  $\frac{1}{2}$  of the wavelength,  $\lambda$ ). The study (as shown in Fig. 1) reveals how the split modes continue to exist despite the change in electrode coverage. Furthermore, the  $Q_{3dB}$ , which accounts for losses due to the PML exhibit a value below 1,500, meaning that the split modes are probably the source of low  $Q$ . Clearly, a different method to excite TSM resonators should be investigated.

### Electrode shaping for energy trapping

It is possible to trap energy at a desired frequency for a particular acoustic mode by looking at the frequency vs. wavenumber (dispersion curve) of various modes occurring in the same plate geometry. The wave solutions for two-dimensional equations of motion of anisotropic plates (AT-cut quartz plates), with transverse shear deformation was presented in [2]. In this case coupling between thickness shear, thickness twist, flexural, and other waves existed. This analysis also showed that the fundamental frequency for a thickness-shear wave can be isolated by appropriately designing the electrode shape, *i.e.* trapping the energy only in the fundamental mode. The design methodology for energy trapping or electrode shaping was presented by Mindlin in [3]. We followed this methodology to design the electrode shape for Y-cut LN thin film and used stiffness, piezoelectric and dielectric coefficients of the Y-cut LN (after properly rotating the standard Z-cut LN coefficients). Because of the anisotropy of the material, the electrode length,  $L$ , becomes a function of the X-Z direction and should be kept below a specific value:

$$L = 2h\pi \sqrt{\frac{\left(\frac{1}{3}\alpha + \frac{\gamma_{22}}{3\kappa^2 c_{44}}\right) \cos^2 \varphi + \frac{\gamma_{66}}{3\kappa^2 c_{44}} \sin^2 \varphi}{2\left(R + \frac{4k_{34}^2}{\pi^2}\right)}} \quad (1)$$

$$k_{34}^2 = \frac{e_{34}^2}{c_{44}\epsilon_{33} + e_{34}^2} \quad \gamma_{22} = c_{22} - \frac{c_{23}^2}{c_{33}} \quad \gamma_{66} = c_{66} - \frac{c_{56}^2}{c_{55}}$$

$$k^2 = \frac{\pi^2 \left(1 + R - \frac{8k_{34}^2}{\pi^2}\right) (1 + k_{34}^2)}{12}$$

$$R = \frac{\rho_{Al} h_{Al} + \rho_{Pt} h_{Pt}}{\rho_{LN} h_{LN}} \quad \alpha = \frac{1 + 3R}{1 + R}$$

where  $h$  is the thickness of the plate (in the Y-axis),  $\varphi$  is the angle between X and Z axis of the Y-cut LN plate,  $R$  is the ratio of the mass per unit area of both electrodes (in this case, aluminum and platinum) to the mass per unit area of the Y-cut LN plate.  $\kappa$  is the shear correction factor including the contributions of both the mass of the electrodes and the piezoelectric effect,  $\gamma_{22}$  and  $\gamma_{66}$  are the Voigt's stretch modulus of the plate,  $c_{ij}$  are the  $ij$  stiffness constants,  $\epsilon_{33}$  is the 33 dielectric constant,  $e_{34}$  is the 34 piezoelectric coefficient and  $k_{34}^2$  is the associated electromechanical coupling.

Figure 2 shows the electrode shape obtained by following Eq. (1) and results in a maximum extension of 47  $\mu\text{m}$  along Z and minimum of 21  $\mu\text{m}$  along the X-axis. We selected the largest values of  $L$  so as to maximize the capacitance of the resulting device. These values as well as the selection of the overall plate size of 52  $\mu\text{m}$  x 28  $\mu\text{m}$

were validated by FEM in COMSOL. In Fig. 4, it is clear that the electrode shaping techniques eliminates the split modes and facilitates harnessing the full coupling of the LN thin film technology.

Another technique that we explored for energy trapping is based on the definition of a mesa structure. The mesa is generally implemented by creating a step around the edge of the resonator. We demonstrated this technique in our process by adding a 1  $\mu\text{m}$  thick film of AlN along the longest edges of the rectangular plate (Fig. 3). The width of the AlN mesa was selected to be 1.25  $\mu\text{m}$  by means of FEM analysis (Fig. 4). This value resulted in the most reduced spurious modes. An equally large value of coupling is attained by the mesa structure. This technique offers more flexibility in setting the device static capacitance at the expenses of a slightly reduced coupling. It is also interesting to note that the AlN reflectors cause a slight shift in the center frequency of the device.

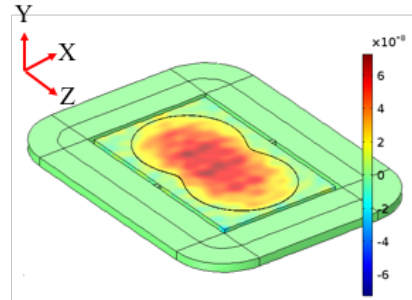


Figure 2: 3D COMSOL simulation showing total displacement for the electrode shape design in the Y-cut LN film. An anchor size of 2.5  $\mu\text{m}$  by 2.5  $\mu\text{m}$  was used in this simulation.

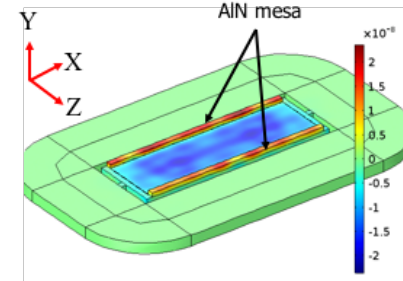


Figure 3: 3D COMSOL simulation showing total displacement for the rectangular shape design with the AlN mesa structure. An anchor size of 2.5  $\mu\text{m}$  by 2.5  $\mu\text{m}$  was used in this simulation.

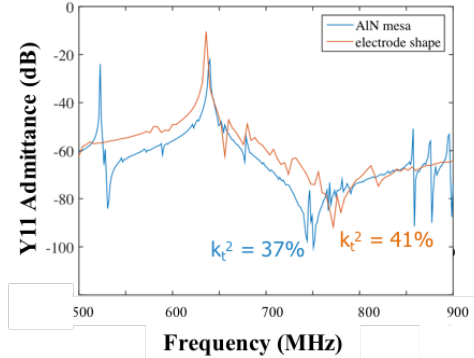


Figure 4. Simulated  $Y_{11}$  response of the electrode shape design and rectangular shape with the AlN mesa. Losses were modeled via PML and are extremely low in this simulation (differently from what recorded experimentally).

## DEVICE FABRICATION

The TSM resonators were fabricated using the process shown in Fig. 5. This process is unique in enabling the definition of Y-cut resonators with a bottom electrode. 100 nm thick Pt is sputtered on lithium niobate (LN) wafer, which is utilized as bottom electrode. This wafer (facing Pt) is bonded with a high resistive Si wafer using room temperature surface activated bonding (SAB) technique. After bonding, the LN wafer is polished down to a thickness of 2.5  $\mu\text{m}$ . A thick photoresist mask is used to pattern the LN and etching is performed using ion milling equipment. The etch rate in ion milling for LN is 24 nm/min and has a 1:1 etch selectivity with the photoresist. The etching is controlled by monitoring the etched materials in a secondary ion mass spectroscopy (SIMS) attached to the ion milling equipment. As the bottom electrode also follows the plate dimensions, the etching is stopped after concluding the etching of Pt. In addition, the anchor definition was also limited due to the Pt overhang. The photoresist is removed in acetone with ultrasonic agitation. 1165 microposit remover solution, heated at 80  $^{\circ}\text{C}$ , is used to remove any surface residues. Later, 1  $\mu\text{m}$  of aluminum nitride is sputtered using Tegal's AC reactive sputtering tool operating at 7 kW. The patterning of the AlN film is done by using a 2  $\mu\text{m}$  thick photoresist. The AlN is etched using  $\text{Cl}_2$  based ICP RIE. The aluminum nitride layer is used as a passivation for routing the wires from the lithium niobate plate, for the pads and for the mesa definitions. However, because of over etch in this step, the width of the AlN mesa was not defined according to the design value and resulted in a non-rectangular cross section. Top electrode (aluminum, 100 nm) and contact/pad fabrication (aluminum, 200 nm) are patterned using a lift-off process.

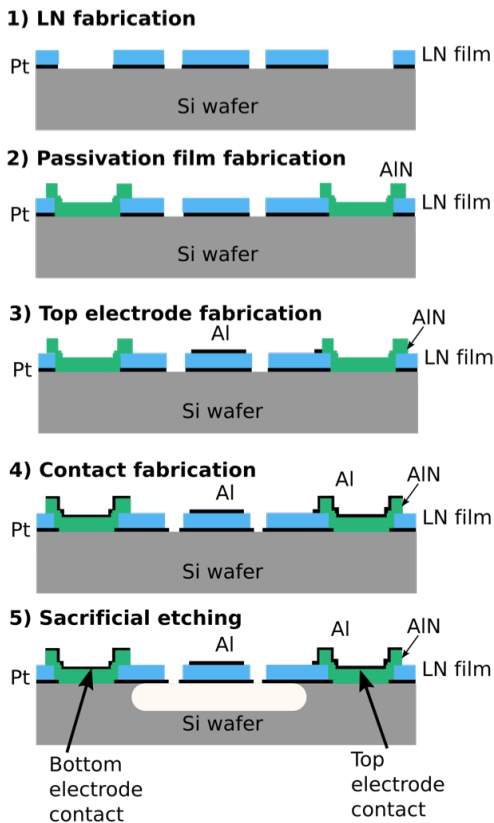


Figure 5: Fabrication process flow.

For lift-off, acetone with ultrasonic agitation is utilized. IPA rinse following Semitool's spin rinser and dryer is used for cleaning the wafer. Finally, the silicon underneath the device area is etched using  $\text{XeF}_2$  vapor phase etching.

## RESULTS AND DISCUSSION

The microscope image of one of the fabricated devices with the designed electrode shape is shown in Figure 6. The sidewall of LN etch definition is roughly  $\sim 70^{\circ}$  (see Figure 7). Figure 8 shows the SEM image of the same device and a zoomed in view of the routing electrodes over the AlN layer in Figure 9. An overhang of the Pt layer is observed because the incident angle to etch Pt (in ion milling) with straight sidewall is not the same as for the LN thin film. Figure 10 shows the SEM image of the device with AlN as a mesa structure. Because of the smaller lengths of the anchors, the anchoring region of these devices resulted in a large Pt overhang. The devices are one port and the bottom electrode is capacitively coupled to ground through the LN film [12]. Their measurement is performed using an Agilent VNA and a GSG150 pitch probe on a Semiprobe probe station. Multiple measured devices with electrode shaping exhibited  $k_t^2$  around 36 % with very limited spurious around the main resonance.

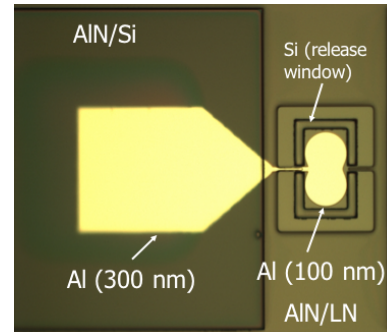


Figure 6. Microscope image of one of the fabricated (unreleased) Y-cut LN thickness shear mode resonators with top (Al) and bottom (Pt) electrode.

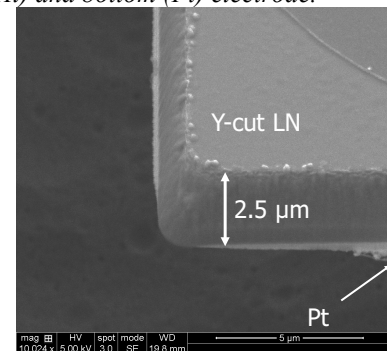


Figure 7. Cross-section of the etched Y-cut LN film.

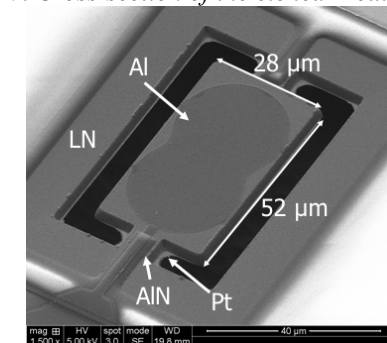


Figure 8. SEM image of the resonator shown in Fig. 6.



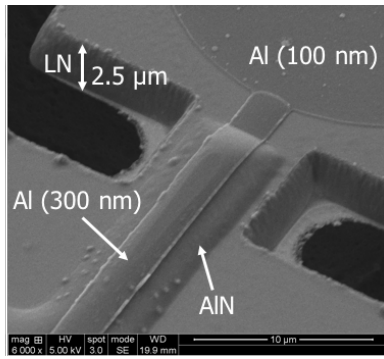


Figure 9. Routing of Al on top of AlN to reduce parasitics.

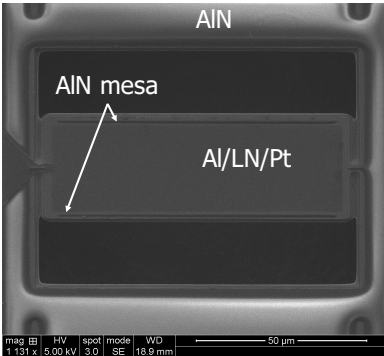


Figure 10. Fabricated device with AlN mesa structure.

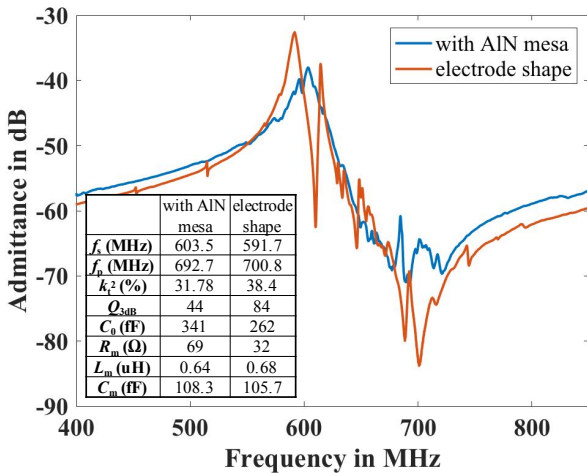


Figure 11. Measured TSM resonator's  $Y_{11}$  response of Figure 8 and 10.

The 3dB  $Q_s$  for these measurements are ranging between 30 and 90. Typical responses for both electrode shaping and with AlN mesa are shown in Figure 11. Although spurious modes are seen between the resonant and antiresonant frequencies, no split modes at the resonant frequency are observed. The sources of the low  $Q$  are unknown at this point and further investigations are required to understand it.

## ACKNOWLEDGEMENT

The material is based upon work supported by the Defense Advanced Research Projects Agency (DARPA) under Contract No. HR0011-15-C-0137. Authors would like to thank the staff of Carnegie Mellon University's Nanofabrication facility for their kind support. Authors would also like to thank Dr. Yuji Hori and Mr. Shigeru Haramatsu of NGK Insulators, Ltd. for providing the thin lithium niobate films.

## REFERENCES

- [1] R.D. Mindlin, P.C.Y. Lee, "Thickness-shear and flexural vibrations of partially plated, crystal plates", International Journal of Solids and Structures, Volume 2, Issue 1, Pages 125-139, 1966.
- [2] R. D. Mindlin and W. J. Spencer, "Anharmonic, Thickness-Twist Overtones of Thickness-Shear and Flexural Vibrations of Rectangular, AT-Cut Quartz Plates", The Journal of the Acoustical Society of America, pp. 1268-1277, Vol 42, 1967.
- [3] R. D. Mindlin, "Optimum Sizes and Shapes of Electrodes for Quartz Resonators", The Journal of the Acoustical Society of America, pp. 1329-1331, Vol. 43, 1968.
- [4] J. Bjurstrom, G. Wingqvist and I. Katardjiev, "Synthesis of textured thin piezoelectric AlN films with a nonzero C-axis mean tilt for the fabrication of shear mode resonators", in IEEE Transactions on Ultrasonics, Ferroelectrics, and Frequency Control, vol. 53, no. 11, pp. 2095-2100, November 2006.
- [5] C. D. Corso, A. Dickherber and W. D. Hunta, "Lateral field excitation of thickness shear mode waves in a thin film ZnO solidly mounted resonator", Journal of Applied Physics 101, 054514, 2007.
- [6] H. Abe, T. Yoshida and H. Watanabe, "Energy trapping of thickness-shear vibrations excited by parallel electric field and its application to piezoelectric vibratory gyroscopes", IEEE Ultrasonics Symposium Proceedings, pp. 467-471 vol.1, 1998.
- [7] I. E. Kuznetsova, et. al, "Investigation of acoustic waves in thin plates of lithium niobate and lithium tantalate", in IEEE Transactions on Ultrasonics, Ferroelectrics, and Frequency Control, vol. 48, no. 1, pp. 322-328, Jan. 2001.
- [8] S. Gong and G. Piazza, "Design and Analysis of Lithium-Niobate-Based High Electromechanical Coupling RF-MEMS Resonators for Wideband Filtering", in IEEE Transactions on Microwave Theory and Techniques, vol. 61, no. 1, pp. 403-414, Jan. 2013.
- [9] R. Wang, S. A. Bhavne and K. Bhattacharjee, "Low TCF Lithium Tantalate contour mode resonators", 2014 IEEE International Frequency Control Symposium (FCS), Taipei, 2014, pp. 1-4.
- [10] A. Kochhar, G. Vidal-Álvarez, L. Colombo, and G. Piazza, "Integration of bottom electrode in Y-cut lithium niobate thin films for high electromechanical coupling and high capacitance per unit area MEMS resonators", IEEE 30th International Conference on Micro Electro Mechanical Systems (MEMS), pp. 962-965, 2017.
- [11] W. P. Mason, "Physical Acoustics, Principles and Methods", Volume 16, Chapter 2, pp. 37 – 171, 1982.
- [12] A. Kochhar, G. Vidal-Álvarez, L. Colombo and G. Piazza, "High coupling two-port lithium niobate MEMS resonators using capacitive ground concept", 2017 IEEE International Ultrasonics Symposium (IUS), Washington, DC, USA, 2017, pp. 1-4.

## CONTACT

\*Abhay Kochhar; abhay.kochhar@ieee.org